2022

Hybrid Heat Pump Controls: Conventional Dual Fuel versus Seamlessly Fuel Flexible Heat Pump

Zhenning Li

Kyle Gluesenkamp

Bo Shen

Jeffrey Munk

Helia Zandi

See next page for additional authors

Hybrid Heat Pump Controls: Conventional Dual Fuel versus Seamlessly Fuel Flexible Heat Pump

Zhenning Li[1], Kyle Gluesenkamp[1]*, Bo Shen[1], Jeffrey Munk[1], Helia Zandi[1], Praveen Cheekatamarla[1], Steve Kowalski[1]

[1]Oak Ridge National Laboratory, Oak Ridge, TN, 37830 USA
Email: liz5@ornl.gov, gluesenkampk@ornl.gov, shenb@ornl.gov, munkjd@ornl.gov, zandih@ornl.gov ,cheekatamapk@ornl.gov, kowalskisp@ornl.gov

ABSTRACT

This paper compares the performance of a novel seamlessly fuel flexible heat pump (SFFHP) and conventional dual fuel heat pump (DFHP) for space heating. The conventional dual fuel systems either run on the gas furnace or electric heat pump at any given moment, as a comparison, the proposed seamlessly fuel flexible heat pump simultaneously consumes gas and electricity by continuously optimizing the proportion of each. The process air flows across the heat pump condenser first and then flows across the furnace coil, therefore, the heat pump temperature lift is reduced. SFFHP delivers energy savings by allowing each subsystem, i.e., gas furnace and electric heat pump, to operate where it performs best.

For DFHP, two operation control strategies, i.e., non-restricted control and restricted control, are available on market. For the non-restricted mode, the thermostat has a switching temperature-programmed according to the balancing point of heating load and capacity curve. Heat pump operates above the switching temperature, while the furnace takes over under the switching temperature. For the restricted control, the compressor of a heat pump is disabled below a predefined lockout outdoor temperature to let the furnace take over. For SFFHP, a model predictive control strategy is developed to continuously adjust the capacities of the electric heat pump and gas furnace based on the foreseen weather data, utility price signals, and marginal grid emission signals with the goal of minimizing the utility cost and CO_2 emission while guaranteeing comfort requirements.

In this paper, DFHP and SFFHP are simulated using high-fidelity heat pump performance curves generated from DOE/ORNL heat pump design model. Performance comparison of DFHP and SFFHP during 2019-2020 heating season in Los Angeles shows that SFFHP with model predictive control achieves 23% utility cost reduction and 17 % CO_2 emission reduction. Case studies demonstrate that SFFHP can deliver significant reductions in peak demand, utility cost, and CO_2 emission. As a result, SFFHP can deliver superior benefits for utility cost reduction and CO2 emission reduction over conventional dual fuel heat pump.

Key words: Dual fuel, Heat Pump, Furnace, Fuel flexible, Model predictive control

1. INTRODUCTION

In response to global warming and climate change, United States has implemented related policies and technical efforts that include the use of renewable energy and the increase of energy efficiency to reduce energy consumption and greenhouse gas (GHG) emissions. The first executive order signed by President Joe Biden's administration in 2021 streamlined the milestones to reduce the carbon footprint of the US building stock by 50% before 2035 and ensure the US achieves a 100% clean energy economy and reaches net-zero emission society no later than 2050. Although the ultimate carbon reduction goal is to eliminate fossil fuels, it is vitally important to increase the efficiency of existing fossil fuel-based building equipment in the transition period to zero emissions. The more effective use of existing fuel powered device will allow significant reductions in GHG emissions and energy waste. One promising equipment which shows good compromise between economic and environmental impacts in the transition period is the dual fuel heat pump (DFHP) consisting of an electric heat pump (HP) and a natural gas furnace Yu *et al.* (2019).

For a conventional DFHP, during extreme cold weather when the HP capacity and efficiency drop, auxiliary heat is provided by a fossil-fuel furnace. The furnace kicks in when the outdoor temperature reaches the balance point where it is cheaper to fire up the furnace than operate the HP at low efficiency and low capacity. Depending on the HP and heating load of the space, this balance or switching point usually range from -10 C° to -15 °C. The switching point can either be fixed at the thermostat or at the HP control board. The furnace can be powered by natural gas, oil or propane. HP saves energy because pumping heat uses less energy than producing heat. The efficiency of the advanced furnace ranges from 90 to 96% while recent advances Munk *et al.* (2021) in cold climate heat pump show that HP can achieve 4.5 in terms of coefficient of performance (COP) at 8.3 ° C outdoor temperature, 3.0 COP at -8.3 ° C, 2.5 COP at -15 ° C and 1.8 COP at -26.1 ° C.

The electricity sector has seen a shift from traditional centralized system to a smart grid device Alibabaei *et al.* (2017). This phenomenon has been ushered in by the increased integration of renewable energies. The rapid proliferation of the 'Internet of Things' (IoT) Siano (2014) allow major loads, such as heat pumps, to be controlled with the goal of reducing peak power consumption on the electrical grid. In a smart grid, heat pumps can be considered part of the demand side that can be actively managed to stabilize voltage fluctuations caused by high demand or high penetration of renewable energy Fischer and Madani (2017). With smart control of dual fuel heat pump, the system can switch between furnace and heat pump mode depending on the outdoor temperature, gas and electricity prices, desired indoor temperature, renewable energy generation and heat pump's COP Siano (2014). The smart switching controls between furnace and EHP have been conducted in literature Demirezen and Fung (2021), in which, a Smart Dual Fuel Switching System (SDFSS) prototype was built and demonstrated that it was capable to reduce GHG emissions and optimize the HVAC equipment's energy cost when the system was regulated by model predictive control (MPC).

It is important to describe how to incorporate a grid's GHG (greenhouse gases) condition into a site-specific MPC. The grid system-wide emission rate in a specific grid region depends on the total power production rate from grid power generators, and other factors that affect system operating conditions, such as weather. The marginal operating emissions rate (MOER) is the partial derivative of the systemwide emission rate with respect to the total production rate Callaway *et al.* (2018). It means the change of the emission rate in the grid region with respect to the last megawatt produced by dispatchable generators having the unit of metric Ton CO2-equivalent per MWh [mTonCO2e/MWh]. Intuitively, this indicates how much carbon emission rate increases/decreases in a grid region when one consumes one megawatt more/less. Therefore, MOER allows for associating the power usage at a specific site with the carbon emission rate in the grid region by simply multiplying the on-site power consumption with the MOER signal.

In this paper, we used the MOER signal calculated by WattTime, based on a proprietary model that extends the basic methodology used by Siler-Evans *et al.* (2013) and Callaway *et al.* (2018), but adapted for real-time use. WattTime calculates these marginal operating emission rates in real-time, every 5 min using a combination of grid data from the respective ISO and 5 years of historical Continuous Emissions Monitoring System data Agency (2018). Figure 1 shows a demonstration of WattTime data on June 29th 2021 in California.

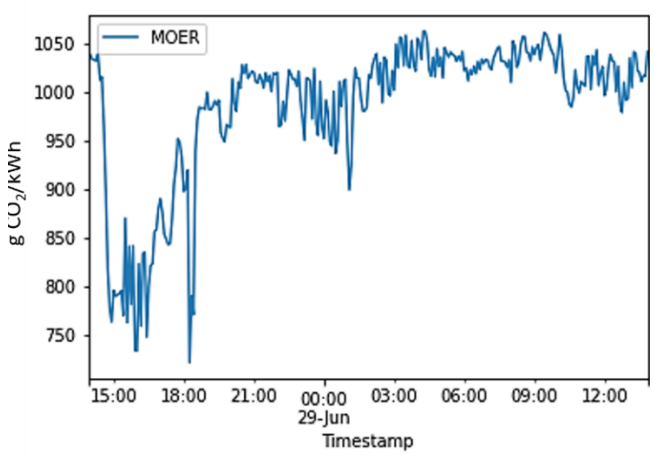

Figure 1: Demonstration of Marginal Grid Emission Data from WattTime (June 29th 2021, California)

Whereas conventional dual fuel systems either run on gas or electricity at any given moment, this study introduces a novel hybrid fuel heat pump which simultaneous consumes gas and electric power. It continuously optimizes the proportion of each, and thus, is called the Seamlessly Fuel Flexible Heat Pump (SFFHP). SFFHP uses IoT technology to adjust the capacities of the electric heat pump and gas furnace continuously based on utility price signals, fuel cost, weather data, and equipment modeling results. By heating the process air first across the heat pump condenser, and then across the furnace coils, the heat pump temperature lift is reduced. This delivers energy savings by allowing each subsystem (gas furnace and electric heat pump) to operate where it performs best. Figure 2 shows the schematic of Seamlessly Fuel Flexible Heat Pump.

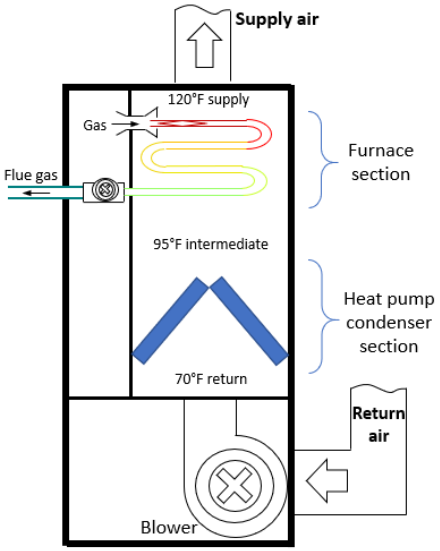

Figure 2: Schematic of Seamlessly Fuel Flexible Heat Pump (SFFHP)

2. METHODOLOGY

SFFHP uses several different parameters such as weather data, natural gas price and electricity utility pricing, equipment performance predicted by the system model to regulate its operation. This research develops multi-objective control optimization to regulate the heating capacity of furnace and EHP in a small time frame with the goal of saving operational cost and reducing GHG emission. As shown in Figure 3, SFFHP is grid-responsive appliance capable of deciding the most cost-effective and environment-friendly operation strategy.

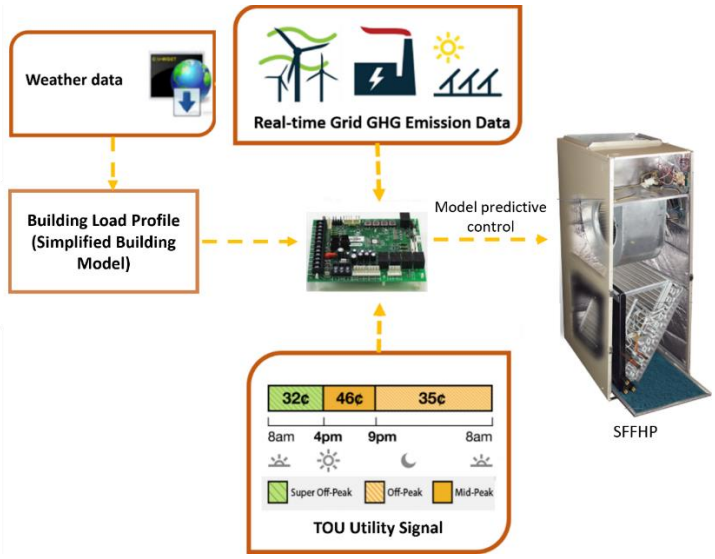

Figure 3: Optimal model-based control architecture of SFFHP

2.1 System Simulation Model

The DOE/ORNL Heat Pump Design Model (HPDM) is used to model the performance of an air-conditioning system. The HPDM is a public-domain HVAC equipment and system modeling and design tool which supports a free web interface and a desktop version for public use. Some features of the HPDM related to this study are introduced below.

Compressor model: To compare refrigerant performances, it was assumed that the compressor has the same volumetric efficiency (η_{vol}=95% in Equation (1)) and isentropic efficiency ($\eta_{isentropic}$=70% in Equation (2)).

$$m_r = Volume_{displacement} \times Speed_{rotation} \times Density_{suction} \times \eta_{vol}, \quad (1)$$

$$Power = m_r \times (h_{\text{discharge,s}} - h_{\text{suction}}) / \eta_{isentropic}, \quad (2)$$

where m_r is compressor mass flow rate; *Power* is compressor power; η_{vol} is compressor volumetric efficiency; $\eta_{isentropic}$ is compressor isentropic efficiency; h_{suction} is compressor suction enthalpy; $h_{\text{discharge,s}}$ is the enthalpy obtained at the compressor discharge pressure and the suction entropy; and $Speed_{rotation}$ is the motor rotational speed.

Heat exchanger model: A finite volume (segment-to-segment) tube-fin HX model is used to simulate the performance of the HX with different circuitries. This model has been validated by the experiment data from Abdelaziz et al. (2016).

Expansion device: Isenthalpic process is assumed in the expansion process.

Fans: The airflow rate and power consumption are direct inputs from the laboratory measurements for the model calibrations.

Refrigerant Lines: Temperature changes and pressure drops in suction, discharge, and liquid lines are specified using the measured data from the experiments.

Refrigerant Properties: REFPROP version 10.0 (Lemmon *et al.* (2010) is used to simulate the new refrigerant mixtures by making the mixture definition file according to the required format.

For more details on the HPDM, see Shen and Rice (2016).

In this study, a 3-ton cold climate heat pump is used as the sub-system of SFFHP. The rated heating capacity is 10.55 kW in heating mode and 10.64 kW in cooling mode under AHRI 210/240 test standards. This model is validated against experiment data (Munk, Shen, and Gehl 2021). The natural gas furnace is a commercial product with 1200 CFM as maximum air flow rate and 95% as the rated Annual Fuel Utilization Efficiency (AFUE). The natural gas energy density used in the simulation is 10.395 kWh/m^3.

2.2 Optimization Problem Formulation

Genetic Algorithm (GA) implemented in MATLAB is used to solve the capacity distribution of the two sub-systems, i.e., electric heat pump and furnace, at each time step. The two objectives of optimization are to minimize the utility cost of heating season and minimize the total CO_2 emission as shown in Equation (1).

$$Objective-1: Minimize(\sum_{t=Start\ of\ Heating\ Season}^{End\ of\ Heating\ Season} Utility\,\mathrm{Cost}(t))$$
$$Objective-2: Minimize(\sum_{t=Start\ of\ Heating\ Season}^{End\ of\ Heating\ Season} GHG\ Emission(t)) \quad (1)$$

Equation (2) calculates the utility cost at each moment of a day. In Equation (2), $Ratio_{HPtoTotal}$ is the design variable in the optimization problem. $Ratio_{HPtoTotal}$ refers to the ratio between the capacity of heat pump to the total capacity of SFFHP. $Q_{building}(t)$ is the building heating load obtained from EnergyPlus (Crawley *et al.* (2001)), $COP_{HP}(t)$ is the coefficient of performance of electric heat pump predicted by HPDM. $price_{electricity}$ and $price_{naturalGas}$ is the Time-of-Use electric price and natural gas price, respectively. η is the furnace efficiency.

$$Utility\,\mathrm{Cost}(t) = \frac{Ratio_{HPtoTotal} \times Q_{building}(t)}{COP_{HP}(t)} \times price_{electricity}(t) + \frac{(1-Ratio_{HPtoTotal}) \times Q_{building}(t)}{\eta_{furnace}} \times price_{Natural Gas} \quad (2)$$

Similarly, the emission at each time step is calculated in Equation (3). The first term on the right side of Equation (3) is the emission of heat pump and the second term is the emission of furnace. $Emission_{GridMarginal}(t)$ is the marginal emission grid signal from WattTime. $Emission_{NaturalGasPerkWh}(t)$ is the gas emission density, i.e., 179.6 gCO_2/kWh.

$$Emission(t) = \frac{Ratio_{HPtoTotal} \times Q_{building}(t)}{COP_{HP}(t)} \times Emission_{GridMarginal}(t) + \frac{(1-Ratio_{HPtoTotal}) \times Q_{building}(t)}{\eta_{furnace}} \times Emission_{NaturalGasPerkWh} \quad (3)$$

The multi-objective optimization is conducted using weighted sum method. Equation (4) shows how to calculate the fitness value of a control strategy. The w_1 and w_2 are weights specified by the user. The relative values of the weights reflect the different priorities of different objectives. The optimal designs are achieved through minimizing the fitness value. Because the weighted sum method depends on comparing the values of different objectives, those values usually have different units and/or different orders of magnitude. It is necessary to normalize the objectives. Equation (4) also shows how to normalize the utility cost and the emission.

$$Normalized\ \ Objective-1: Utility\,\mathrm{Cost}^{norm} = \frac{Utility\,\mathrm{Cost}(Ratio_{HPtoTotal}) - Utility\,\mathrm{Cost}_{\min}}{Utility\,\mathrm{Cost}_{\max} - Utility\,\mathrm{Cost}_{\min}}$$
$$Normalized\ \ Objective-2: CO2Emission^{norm} = \frac{CO2Emission(Ratio_{HPtoTotal}) - CO2Emission_{\min}}{CO2Emission_{\max} - CO2Emission_{\min}}$$
$$fitness = w_1 \times Utility\,\mathrm{Cost}^{norm} + w_2 \times CO2Emission^{norm} \quad (4)$$
$$where\ w_1 + w_2 = 1$$

The upper and lower bounds of utility cost and emission amount cannot be known before running the optimization; however, the approximated values of those limits are sufficient to maintain the objectives in the same order of magnitude (Arora (2004). In this study, those upper and lower limits are obtained by preliminary optimization runs.

2.3 Case Study

The performance of SFFHP is first evaluated using Los Angeles TMY-3 weather data from November 1st, 2019, to February 29th, 2020. Figure 4 shows dry bulb temperature at each hour of these 4 months. The thermostat set temperature is specified as 65 °F in heating season.

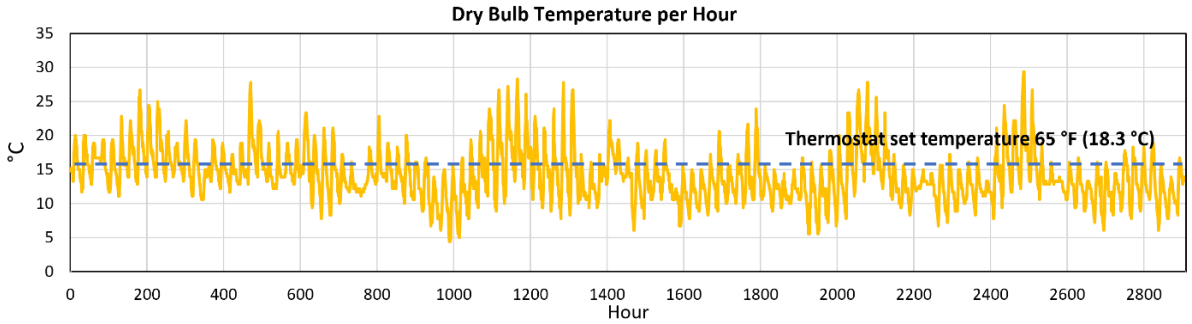

Figure 4: Dry Bulb Temperature for Each Hour of Los Angeles from November 2019 to February 2020

Figure 5 shows the marginal grid emission data from November 2019 to February 2020 for the area administrated by Los Angeles Department of Water and Power.

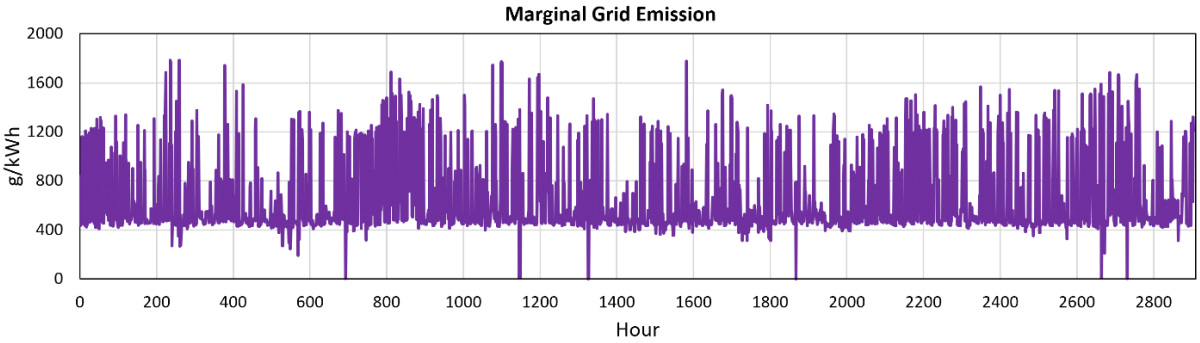

Figure 5: Marginal Grid Emission for Each Hour of Los Angeles from November 2019 to February 2020

Time-of-Use utility rate is adopted from Southern California Edison (SCE) and the natural gas price is adopted from SoCalGas (Figure 6). The electricity price ranges from 25 to 44 cents per kWh, while the gas is only 4.27 cents per kWh.

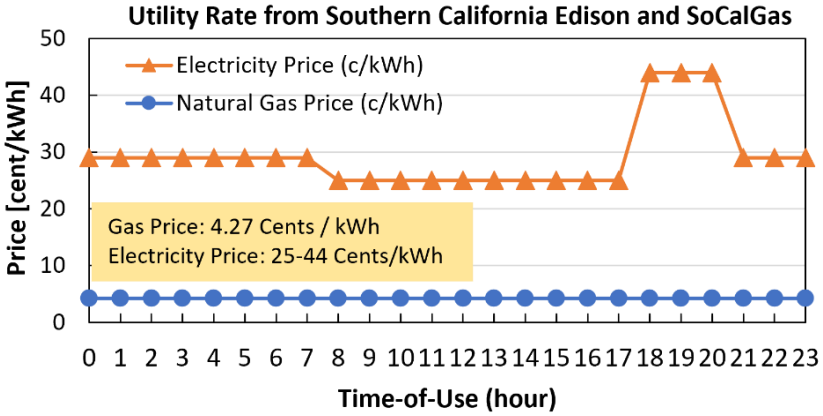

Figure 6: Time-of-Use Utility Rate from Southern California Edison (SCE) and Gas Price from SoCalGas

Figure 7 shows the Pareto Front for the optimal performance of SFFHP operated under the model-based control strategy. Different performance points represent different operation strategies for SFFHP by varying the weights on the two objectives, i.e., either to be more emission-reduction oriented or to be more operation-cost-reduction oriented. As indicated by the Pareto Front, running furnace alone is the cheapest option due to the significant lower gas price. Two performance points, 'Opt-medium' and 'Opt-LowCO_2', are sampled from the Pareto Front. Opt-medium is in the middle of Pareto Front, and it has compromised performance between utility saving and emission reduction, while Opt-LowCO_2 yields the most significant CO_2 emission reduction. Compared with a conventional heat pump, when SFFHP is operated under 'Opt-medium' control strategy, it yields 22.9% utility cost saving with only 2.5% more CO_2

emission. When SFFHP operated under 'Opt-LowCO_2' strategy, it yields 4.2% utility cost reduction and 17.3% CO_2 emission reduction compared with the electric heat pump.

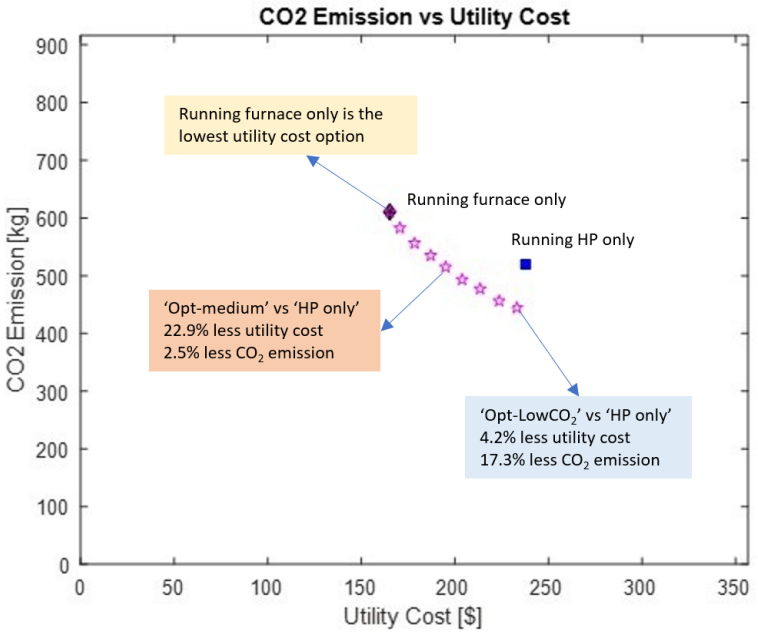

Figure 7: Pareto Front for SFFHP Performance Operated using the Optimal Control Strategies in Los Angeles

To get more insights on the results and investigate the daily performance of the system, the coldest day in heating season is further analyzed. Figure 8 shows the outdoor dry bulb temperature in Los Angeles on December 12th, 2019. The average temperature is 9.6 °C. Figure 9 shows the marginal grid emission of that day for each hour.

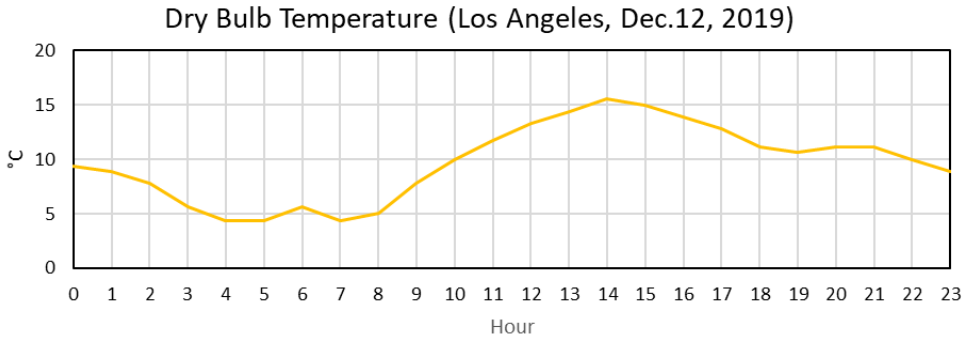

Figure 8: Outdoor Dry Bulb Temperature in Los Angeles, Dec. 12th, 2019

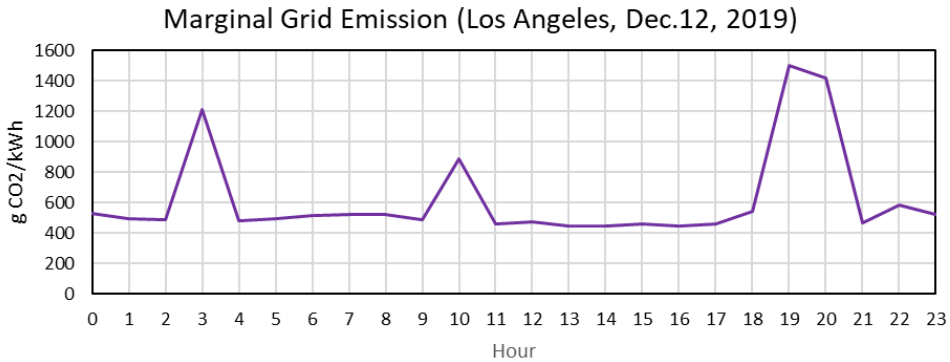

Figure 9: Marginal Grid Emission in Los Angeles, Dec. 12th, 2019

The hourly utility cost of SFFHP is shown in Figure 10. In the morning, the operation cost of heating device is generally higher due to the low outdoor temperature as shown in Figure 8. Running the heat pump alone shows the largest cost, and running the furnace alone shows the lowest cost due the significant price difference between electricity and gas. The utility cost of the SFFHP under two control strategies are between the cost of furnace and heat pump.

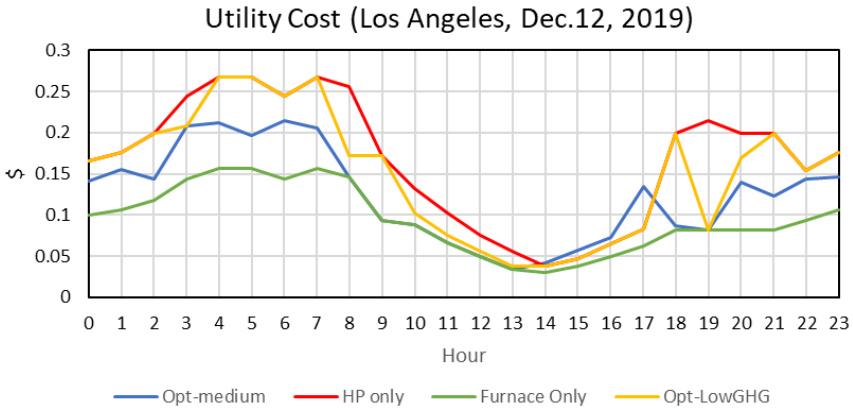

Figure 10: Hourly Operation Cost of SFFHP in Los Angeles, Dec. 12th, 2019

Figure 11 shows the hourly CO_2 emissions of different systems. The Opt-LowGHG operation strategy of SFFHP yields the lowest emission. The peak emission of heat pump matches with the marginal grid emission peaks as seen in Figure 9, since heat pump only consumes electricity. And SFFHP operated under either optimal control strategies can effectively shave the emission peaks by consuming gas during the grid emission-intensive period. This demonstrates the capability of SFFHP for peak demand reduction.

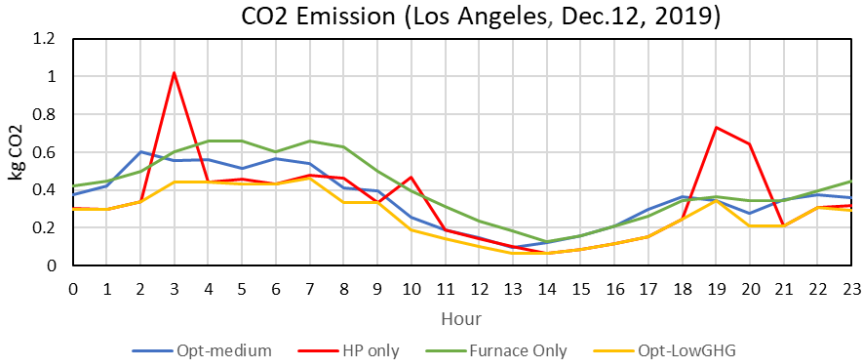

Figure 11: Hourly CO2 Emission in Los Angeles, Dec. 12th, 2019

2.4 Comparison of SFFHP with conventional dual fuel heat pump under different control strategies

To compare performance of SFFHP with conventional dual fuel heat pump under different control strategies, heating season energy consumption simulation using the weather data in Chicago 2019 is used. The performances of three appliances, i.e., DFHP, SFFHP and furnace, are compared. For DFHP, two operating modes are investigated, one mode uses -10 °C switching temperature between furnace and gas, the other mode uses 0 °C as the switching temperature. Figure 12 shows the gas consumptions of different systems. It can also be observed that lower switching temperature induces lower gas consumption for DFHP due to the fewer hours of a year the furnace will operate. When the control strategy is more emission reduction oriented, the gas consumption of SFFHP decreases.

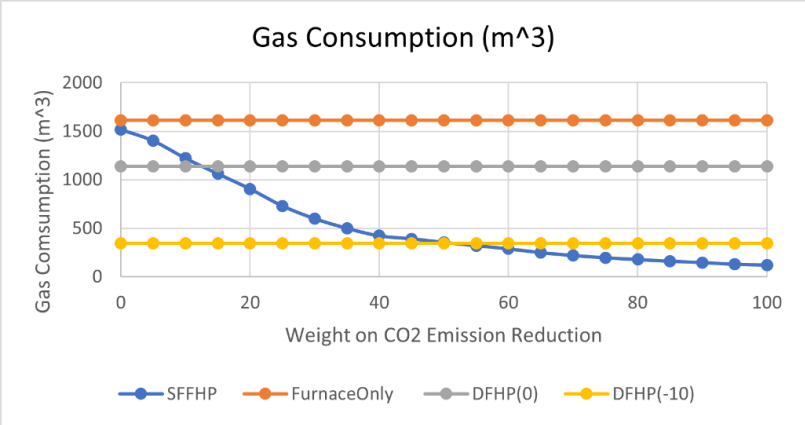

Figure 12: Comparison of annual gas consumption among SFFHP, DFHP and furnace only

Figure 13 shows the CO_2 emission comparison. Similar as gas consumption, emission of SFFHP decreases with the increase of the emission reduction weight. However, DFHP with -10 °C switching temperature has highest emission, this is because when the heat pump operates in low temperature, the COP of heat pump is so low that the emission induced by power generation is larger than natural gas combustion given the same heating capacity.

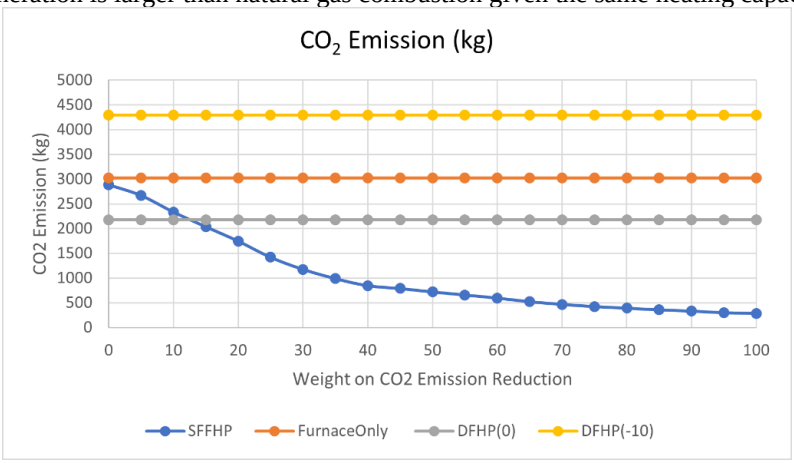

Figure 13: Comparison of annual CO2 emission among SFFHP, DFHP and furnace only

Figure 14 shows the electricity consumption of the three systems. The electricity consumption of SFFHP increases with the weight on emission reduction. The power consumption of SFFHP can be larger than DFHP in exchange of great emission reduction.

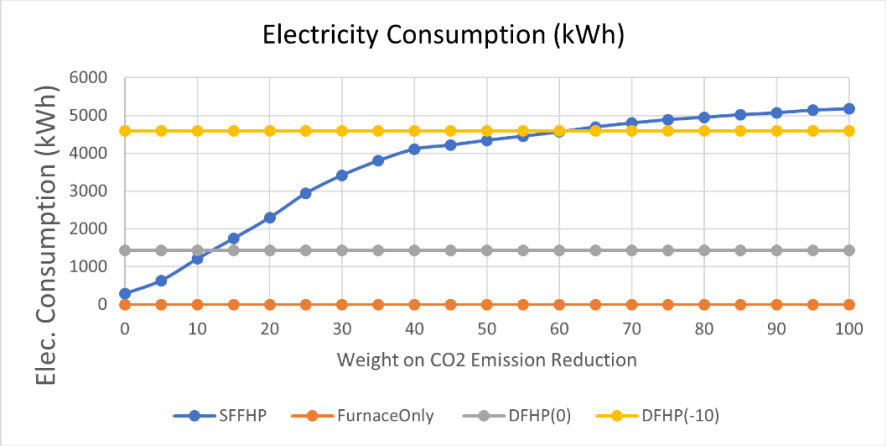

Figure 14: Comparison of electricity consumption among SFFHP, DFHP and furnace only

3. CONCLUSION

This paper introduces a novel hybrid fuel heat pump, i.e., Seamlessly Fuel Flexible Heat Pump (SFFHP), which simultaneously consumes gas and electricity and continuously optimizes the proportion of each. SFFHP accounts for the balance between economic and environmental impacts of the residential and small commercial space heating equipment.

To regulate the operation of SFFHP, various temporal inputs such as TOU electricity price, gas price, the efficiency of electric heat pump, the efficiency of natural gas furnace and the marginal grid emission signal are used to develop the model-based control strategy. Case studies demonstrate that when SFFHP is operated under optimal control strategies, it can deliver up to 23% utility cost reduction and up to 17 % CO_2 emission reduction in Los Angeles. Case studies demonstrate the efficacy of SFFHP for significant reductions in peak demand, utility cost, and CO_2 emission. Due to the hybrid fuel nature of this novel equipment, user comfort will always be maintained, which will lead to a high participation rate of customers in Demand Response (DR) programs.

4. REFERENCES

Abdelaziz, O., S. Shrestha, B. Shen, A. Elatar, R. Linkous, W. Goetzler, M. Guernsey and Y. Bargach (2016). "Alternative Refrigerant Evaluation for High-Ambient-Temperature Environments: R-22 and R-410A Alternatives for Rooftop Air Conditioners." Energy and Transportation Science Division. Oak Ridge National Laboratory. ORNL/TM-2016/513.

Agency, U. E. P. (2018). Air markets program data, US Environmental Protection Agency Washington, DC.

Alibabaei, N., A. S. Fung, K. Raahemifar and A. Moghimi (2017). "Effects of intelligent strategy planning models on residential HVAC system energy demand and cost during the heating and cooling seasons." Applied Energy **185**: 29-43.

Arora, J. S. (2004). Introduction to optimum design, Elsevier.

Callaway, D. S., M. Fowlie and G. McCormick (2018). "Location, location, location: The variable value of renewable energy and demand-side efficiency resources." Journal of the Association of Environmental and Resource Economists **5**(1): 39-75.

Crawley, D. B., L. K. Lawrie, F. C. Winkelmann, W. F. Buhl, Y. J. Huang, C. O. Pedersen, R. K. Strand, R. J. Liesen, D. E. Fisher and M. J. Witte (2001). "EnergyPlus: creating a new-generation building energy simulation program." Energy and buildings **33**(4): 319-331.

Demirezen, G. and A. S. Fung (2021). "Feasibility of Cloud Based Smart Dual Fuel Switching System (SDFSS) of Hybrid Residential Space Heating Systems for Simultaneous Reduction of Energy Cost and Greenhouse Gas Emission." Energy and Buildings **250**: 111237.

Fischer, D. and H. Madani (2017). "On heat pumps in smart grids: A review." Renewable and Sustainable Energy Reviews **70**: 342-357.

HPDM "DOE/ORNL Heat Pump Design Model, https://hpdmflex.ornl.gov."

Lemmon, E. W., M. L. Huber and M. O. McLinden (2010). "NIST standard reference database 23." Reference fluid thermodynamic and transport properties (REFPROP), version **9**.

Munk, J., B. Shen and A. C. Gehl (2021). Cost-Optimized Cold Climate Heat Pump Development and Field Test, Oak Ridge National Lab.(ORNL), Oak Ridge, TN (United States).

Shen, B. and K. Rice (2016). "DOE/ORNL heat pump design model." Web link: http://hpdmflex. ornl. gov.

Siano, P. (2014). "Demand response and smart grids—A survey." Renewable and sustainable energy reviews **30**: 461-478.

Siler-Evans, K., I. L. Azevedo, M. G. Morgan and J. Apt (2013). "Regional variations in the health, environmental, and climate benefits of wind and solar generation." Proceedings of the National Academy of Sciences **110**(29): 11768-11773.

Yu, D., K. Y. Tung, N. Ekrami, G. Demirezen, A. Fung, F. Mohammadi and K. Raahemifar (2019). Proof of Concept of a Cloud-Based Smart Dual-Fuel Switching System to Control the Operation of a Hybrid Residential HVAC System. 2019 IEEE PES Asia-Pacific Power and Energy Engineering Conference (APPEEC), IEEE.